Heliyon 9 (2023) e19503

Contents lists available at ScienceDirect

Heliyon

journal homepage: www.cell.com/heliyon

LncRNA MALAT1 knockdown inhibits the development of choroidal neovascularization

Xiaoli Zhang [a,1], Shu Du [b,1], Defeng Yang [c], Xuemei Jin [b], Yuan Zhang [a], Diya Wang [a], Huixia Wang [b], Yan Zhang [a,**], Manhui Zhu [b,*]

[a] Changchun Aier Eye Hospital, Aier Eye Hospital Group, Changchun, Nanguang District, Jilin Province, China
[b] Department of Ophthalmology, Lixiang Eye Hospital of Soochow University, Suzhou, Jiangsu, China
[c] Department of Ophthalmology, The Second Hospital of Jilin University, Changchun, Jilin, China

ARTICLE INFO

Keywords:
Choroidal neovascularization (CNV)
Metastasis-associated lung adenocarcinoma transcript 1 (MALAT1)
Human choroidal vascular endothelial cells (HCVECs)
Hypoxia

ABSTRACT

In the pathogenesis of age-related macular degeneration, long non-coding RNAs have become important regulators. This study aimed to investigate the role of metastasis-associated lung adenocarcinoma transcript 1 (MALAT1) in the progression of choroidal neovascularization (CNV) and the underlying mechanisms. The in vivo and in vitro model of CNV was established using laser-induced mouse CNV model and human choroidal vascular endothelial cells (HCVECs) exposed to hypoxia respectively. We explore the role of MALAT1 in the pathogenesis of CNV by using the small interference RNA both in vivo and in vitro. MALAT1 expression was found to be upregulated in the retinal pigment epithelial-choroidal complexes. MALAT1 knockdown inhibited CNV development and leakage in vivo and decreased HCVECs proliferation, migration, and tube formation in vitro. MALAT1 performed the task as a miR-17-5p sponge to regulate the expression of vascular endothelial growth factor A (VEGFA) and E26 transformation specific-1 (ETS1). This study provides a new perspective on the pathogenesis of CNV and suggests that the axis MALAT/miR-17-5p/VEGFA or ETS1 may be an effective therapeutic target for CNV.

1. Introduction

The most common cause of irreversible central vision loss in people over 60 years in developed countries is age-related macular degeneration (AMD). Choroidal neovascularization (CNV), an advanced AMD, can seriously impair vision [1]. Currently, the leading treatment for CNV is intravitreal injection of anti-vascular endothelial growth factor (VEGF) agents. However, within the first four years of treatment, some patients exhibit drug resistance to the anti-VEGF agents [2]. The high costs and long-term injection heavily burden patients. Therefore, exploring the pathogenesis of CNV seems urgent and more effective.

According to studies, long non-coding RNA (lncRNA) is thought to play a key role in the pathogenesis of CNV [3–6]. Metastasis-associated lung adenocarcinoma transcript 1 (MALAT1), a lncRNA, has been linked to both the function of vascular endothelial cells (ECs) and the process of neovascularization formation [7]. Early-onset preeclampsia (EOPE) tissues have lower MALAT1 expression. MALAT1 promotes EC proliferation, migration, and tube formation in an in vitro model of EOPE through

* Corresponding author. Department of Ophthalmology, Lixiang Eye Hospital of Soochow University, Suzhou, Jiangsu, China.
** Corresponding author. Changchun Aier Eye Hospital, Aier Eye Hospital Group, Changchun, Nanguang District, Jilin Province, China.
E-mail addresses: zhangyan1@aierchina.com (Y. Zhang), zhumanhuieye@126.com (M. Zhu).
[1] Xiaoli Zhang and Shu Du contributed equally to this study.

https://doi.org/10.1016/j.heliyon.2023.e19503
Received 28 May 2023; Received in revised form 20 August 2023; Accepted 24 August 2023
Available online 4 September 2023

sponging miR-26a/miR-26b. MALAT1 knockout inhibited ECs angiogenesis by reducing PFKFB3-driven glycolysis [8]. MALAT1 has been shown to induce the growth of vasculogenic mimicry and angiogenesis by promoting tumorigenicity and metastasis in gastric cancer [9]. In mouse retinas, MALAT1 inhibition reduced EC proliferation and neonatal retina vascularization [7]. Several studies have also discovered that MALAT1 is essential for the pathogenesis of diabetes-induced microvascular dysfunction. In the model of diabetic retinopathy, MALAT1 knockdown could reduce microvascular leakage, capillary degeneration, and retinal inflammation. Additionally, MALAT1 knockdown inhibited the retinal endothelial cells from proliferation, migration, tube formation, and endothelial mesenchymal transition under high glucose conditions [10,11]. The possibility that MALAT1 is involved in CNV formation and the underlying mechanism is unknown. Therefore, this study aimed to investigate the function of MALAT1 in the pathogenesis of CNV and its potential mechanism. In the present study, we explore the role of MALAT1 both in vitro and in vivo models of CNV. Bioinformatics prediction, luciferase reporter assay and co-transfection assay were performed to confirm the specific mechanism of MALAT1 in CNV. This study provides a new perspective on the pathogenesis of CNV.

2. Material and methods

2.1. Animals and treatments

The C57BL/6J male mice aged 6–8 weeks were acquired from the animal laboratory of Soochow University. These mice were approved under standard pathogen-free conditions. The animal research ethics committee of Lixiang eye hospital of Soochow University (SLKY2022201) approved all animal experiments. A 33G needle was used to inject MALAT1-short hairpin RNA (shRNA) or MALAT1-scramble shRNA intravitreally two weeks prior to the induction of CNV.

2.2. Laser-induced CNV model in mouse

Pentobarbital sodium (Tocris, USA; 2% w/v) was intraperitoneally injected into the C57BL/6J mice as anesthesia. The next step was to dilate the pupils using tropicamide (0.5%; Alcon, USA). A PASCAL diode ophthalmic laser system (Topcon Medical Laser Systems, Livermore, CA, USA) was used to create four laser spots with a diameter of 50 μm around the optic disc at the 3 h, 6 h, 9 h, and 12 h for laser photocoagulation. The laser had a 150 mW output, a 50 μm, and a 100 ms pulse duration. The presence of bubbles at the photocoagulation point signified a rupture of Bruch's membrane.

2.3. Quantitative real-time polymerase chain reaction (qRT-PCR)

Total RNA of the choroidal tissues and human choroidal vascular endothelial cells (HCVECs) were extracted using the TRIzol® reagent (15596018, Invitrogen, USA). Following the manufacturer's instructions, 1 μg of total RNA to complementary DNA (cDNA) using the Revert Aid First Strand cDNA Synthesis Kit (K1622, Thermo Scientific, USA). qRT-PCR was carried out using SYBR Green Master Mix (A25742, Thermo Scientific) using the Step One Plus RT-PCR system (Foster City, USA). Relative gene expression was calculated using the $2^{-\Delta\Delta CT}$ method. Data displaying the fold change compared to the control group were obtained after normalizing all gene expressions to glyceraldehyde 3-phosphate dehydrogenase (GAPDH). Supplementary Table 1 displays the primer sequences.

2.4. Immunofluorescence

After receiving a certain treatment, the mice were sacrificed, and the retinal pigment epithelial (RPE) complexes were separated from the eyeballs. The RPE complexes were then fixed at room temperature for 2 h in 4% paraformaldehyde (PFA). Following washing, the tissues were blocked at 37 °C for 0.5 h with bovine serum albumin (1%) and TritonX-100 (0.5%). The choroids were spread on glass slides after cutting them into four quadrants. The choroids were incubated at 4 °C overnight with an antibody against isolectin B4 (IB4; I21414, Invitrogen). After 2 h of secondary antibody incubation, the nucleus was stained with 4′, 6-diamino amino-2-phenylindole (DAPI) (D9542, Sigma, MO, USA). A confocal microscope (SP8, Leica, Germany) was used to observe fluorescence.

2.5. Fundus fluorescein angiography (FFA)

Approximately 0.3 ml of 2% sodium fluorescein (2119436, Akron pharmaceuticals, USA) was injected intraperitoneally into mice to identify the area of CNV leakage. The early stage (1–2 min) and late stage (4–5 min) continuous real-time FFA images were collected. Two specialists independently assessed the leakage grade of the CNV using pre-established criteria [12]. Briefly, Grade 0 lesions do not exhibit hyperfluorescence. Hyperfluorescence was found in the Grade I lesion, but no leakage. Early hyper fluorescence and late leakage are both present in Grade IIA lesions. Clinically relevant Grade IIB lesions exhibit increased hyper fluorescence in intensity and size during the transmission phase of angiography.

2.6. Cell culture and treatments

Human Choroidal Microvascular Endothelial Cell Complete Medium (CM-H135, Procell, China) was used to culture HCVECs (Procell, China). Dulbecco's Modified Eagle Medium (11965092, GIBCO, USA) was used to culture HEK-293T cells. The medium was supplemented with 10% fetal bovine serum (26010074, GIBCO), 100 units/mL of penicillin, and 100 mg/mL of streptomycin. Cells

were cultured at 37 °C in a 5% carbon dioxide (CO_2) atmosphere. Cells in the hypoxic group were cultured at 95% nitrogen N_2 and 5% CO_2, while cells in the normal group were cultured at 95% O_2 and 5%CO_2. The small interfering (siRNA) and plasmid were brought from RIBO biology company (RIBOBio, China) and GenePharma (Suzhou, China). The siRNA and plasmid were delivered to cells using Lipofectamine 3000 (L3000015, Invitrogen, USA).

2.7. 5-ethynyl-20-deoxyuridine (EdU) assay

The proliferation of HCVECs was detected following specific treatment using a commercial kit (C10310-1, RIBOBio, China). Briefly, the cells were incubated with EdU-A at 37 °C for 2 h. The cells were then fixed with 4% PFA at room temperature for 30 min. Following a wash, 0.5% Triton X-100 was applied to the cells at room temperature for 15 min. HCVECs were then incubated with DAPI and exposed to the Apollo® reaction cocktail. A fluorescence microscope (SP8, Leica, Germany) was used to observe fluorescence.

2.8. Transwell assay

HCVECs migration was assessed using the Transwell chamber. Briefly, 100 μL of the serum-free medium was supplied after 1×10^4 cells had been seeded in the upper chamber. As a chemoattractant, 300 μL of complete medium was supplied to the bottom chamber. Bottom chamber cells were fixed with 4% PFA and stained with crystal violet following a 48 h incubation at 37 °C (C0121, Beyotime, China). Each sample was counted in four randomly selected fields using an Olympus microscope.

2.9. Tube formation assay

The ice-cold Matrigel Matrix (356234, Corning, USA) was polymerized for 45min at 37 °C immediately after adding it to 24-well plates. Totally, 1×10^5 HCVECs were seeded onto the Matrigel Matrix. Images of the formation of capillary tubes were captured after certain treatments using a light microscope. Analyzing the capillary lengths in each field allowed us to determine the tube formation capacity.

2.10. Western blotting

HCVECs were collected and lysed with protein lysis buffer after receiving a certain treatment. A BCA assay kit (P0012S, Beyotime, China) measured protein concentrations. Protein from each group was separated using sodium dodecyl sulfate-polyacrylamide gel electrophoresis before being transferred to polyvinylidene difluoride membranes in equal amounts. After blocking, the membranes were hybridized with the primary antibodies against VEGFA (ab46154, Abcam, USA) and E26 transformation specific-1 (ETS1) (ab220361, Abcam, USA) overnight at 4 °C. The next day, after washing, the secondary antibody (Abcam, USA) was incubated for 1 h at room temperature. Protein levels were semi-quantified using ImageJ software (NIH, USA), and GAPDH was the loading control.

2.11. Luciferase reporter assay

The wild-type or mutant luciferase reporter genes MALAT1, VEGFA, or ETS1 (which include miR-17-5p binding sites) were cloned downstream of the firefly luciferase gene. HEK-293T cells were simultaneously transfected with miR-17-5p mimics and negative control. Finally, the dual-luciferase reporter assay kit (1980, Promega, USA) was used to measure the luciferase activities.

2.12. Fluorescence in situ hybridization (FISH)

The RIBO biology company (RIBOBio, China) provided the MALAT1 probes. Probes were incubated with HCVECs overnight at 37 °C following pre-hybridization. As cytoplasmic and nuclear controls, 18S and U6 were used. The HCVECs nuclei were counter-stained with DAPI. Image results were obtained using a confocal microscope (SP8, Leica, Germany).

2.13. Statistical analysis

All data are represented as mean ± standard error of the mean. The statistical package for social sciences 22 for Windows was used to perform statistical analysis. Student's t-test (two groups comparisons) or one-way analysis of variance followed by the posthoc Bonferroni test, as appropriate, were used to confirm the difference. All experiments were repeated at least three times. $P < 0.05$ was considered statistically significant.

3. Results

3.1. Knockdown of MALAT1 attenuated CNV lesion in the laser-induced mouse CNV model

The expression of MALAT1 increased on day three and persisted until day seven in the RPE-choroidal complexes after laser photocoagulation (Fig. 1A). Two weeks prior to laser photocoagulation, MALAT1 shRNA or the negative control was intravitreally injected to investigate the biological function of MALAT1 in the CNV formation. MALAT1 expression was decreased, and MALAT1

shRNA2 was selected for subsequent experiments due to its superior knockdown efficiency by injecting MALAT1 shRNA (Fig. 1B). The size of CNV lesions was assessed using histopathological analysis. Seven days after photocoagulation, in the MALAT1 shRNA2 group, the length and thickness of the CNV lesion were reduced, showing a similar effect of the anti-VEGF agent conbercept on the inhibition of CNV (Fig. 1C–E). Phalloidin and IB4 were used to mark the CNV lesions after flat-mounting RPE-choroidal complexes. Similarly, the results showed that MALAT1 knockdown decreased the area of CNV lesion (Fig. 1F–G). FFA was used to detect the vascular leakage of CNV. We showed that the mice in MALAT1 silent group had fewer and smaller vascular leakage areas than controls after seven days of laser photocoagulation (Fig. 1H–I).

3.2. MALAT1 regulates the function of HCVECs in vitro

MALAT1 levels in HCVECs were increased under hypoxic conditions (Fig. 2A). Three sets of siRNA for MALAT1 silencing were designed to determine the impact of MALAT1 in HCVECs. We selected the following research due to the highest silencing efficiency of siRNA1 (Fig. 2B). The ability of HCVECs to proliferate (Fig. 2C–D), migrate (Fig. 2E–F), and form tubes (Fig. 2G–H) was enhanced by hypoxia. However, HCVEC's activities under hypoxia conditions were inhibited by MALAT1 silencing (Fig. 2C–H).

3.3. MALAT1 regulates HCVECs function by acting as a miR-17-5p sponge

LncRNA may function as a miRNA sponge to regulate how miRNAs bind to their target mRNA [13]. The bioinformatics prediction was carried out using Starbase 3.0. We discovered that MALAT1 contains the potential miR-17-5p binding site (Fig. 3A). The results of the FISH assay revealed that MALAT1 was primarily localized in the cytoplasm of HCVECs, with 18S and U6 acting as cytoplasmic and nuclear controls, respectively (Fig. 3B). Next, the downstream of the luciferase gene was cloned with MALAT1 cDNA (MALAT1-WT) and the mutant binding sites with miR-17-5p (MALAT1-MUT). miR-17-5p mimics were used to transfect MALAT1-WT and MALAT1-MUT into HCVECs. miR-17-5p mimic, but not the mimic NC (negative control), significantly inhibited the luciferase activity of MALAT1-WT (negative control). Transfection of a miR-17-5p mimic has no impact on MALAT1-MUT (Fig. 3C). The function of

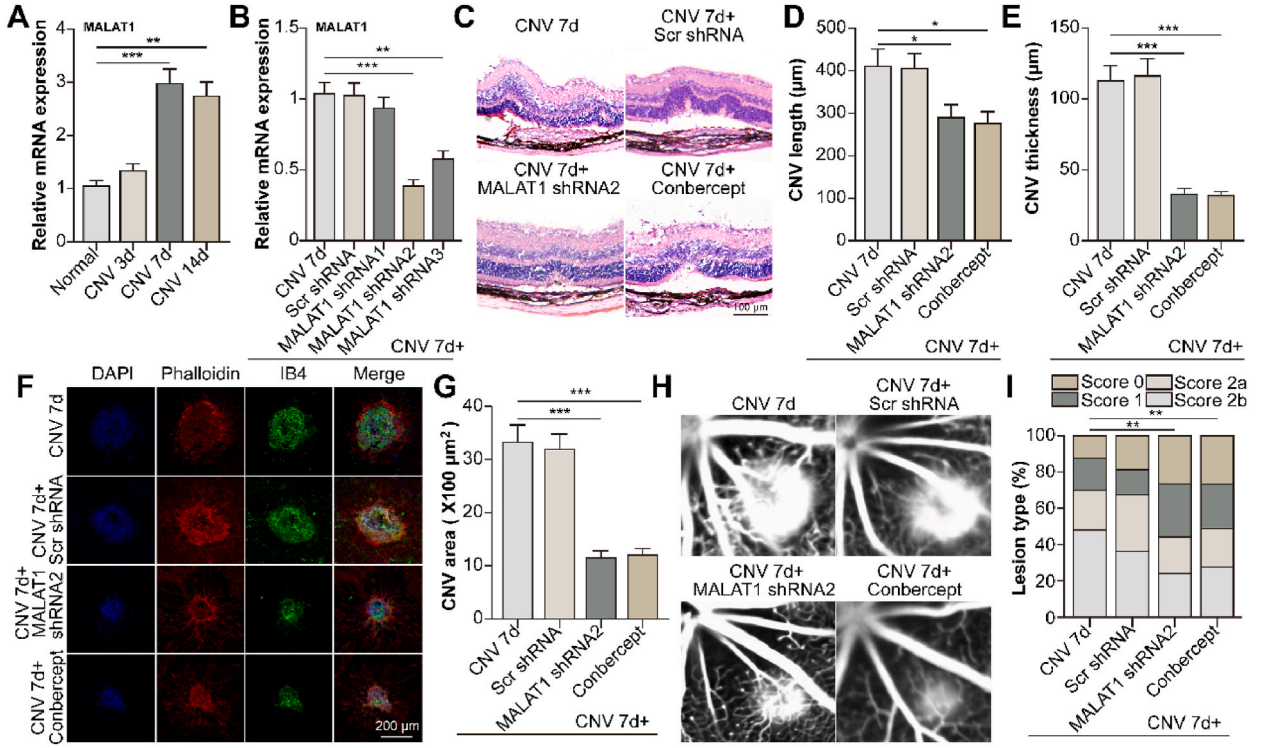

Fig. 1. Knockdown of MALAT1 attenuated choroidal neovascularization (CNV) lesion in the laser-induced mouse CNV model.
(A). Quantitative real-time polymerase chain reaction was used to identify the presence of MALAT1 mRNA in retinal pigment epithelial (RPE)-choroidal complexes. (B). MALAT1 mRNA expression in RPE-choroidal complexes following transfection with MALAT1 short hairpin (shRNA) or scramble shRNA transfection. (C). The hematoxylin and eosin staining images of the CNV 7 d group, CNV 7 d + scramble shRNA, CNV 7 d + MALAT1 shRNA, and CNV 7 d + Conbercept. Conbercept was used as the positive control. Scale bar: 100 μm. (D). Measurement of CNV length. (E). Measurement of CNV thickness. (F). Phalloidin and isolectin B4 were used to stain the choroidal flat mounts of CNV mice, and images of the CNV area were obtained using a confocal laser microscope. Scale bar: 200 μm. (G). Measurement of CNV area. (H). After intraperitoneal fluorescein injection, the fundus fluorescein angiography images of CNV mice were obtained. (I). Graded and quantified angiogenic vessel leakage.

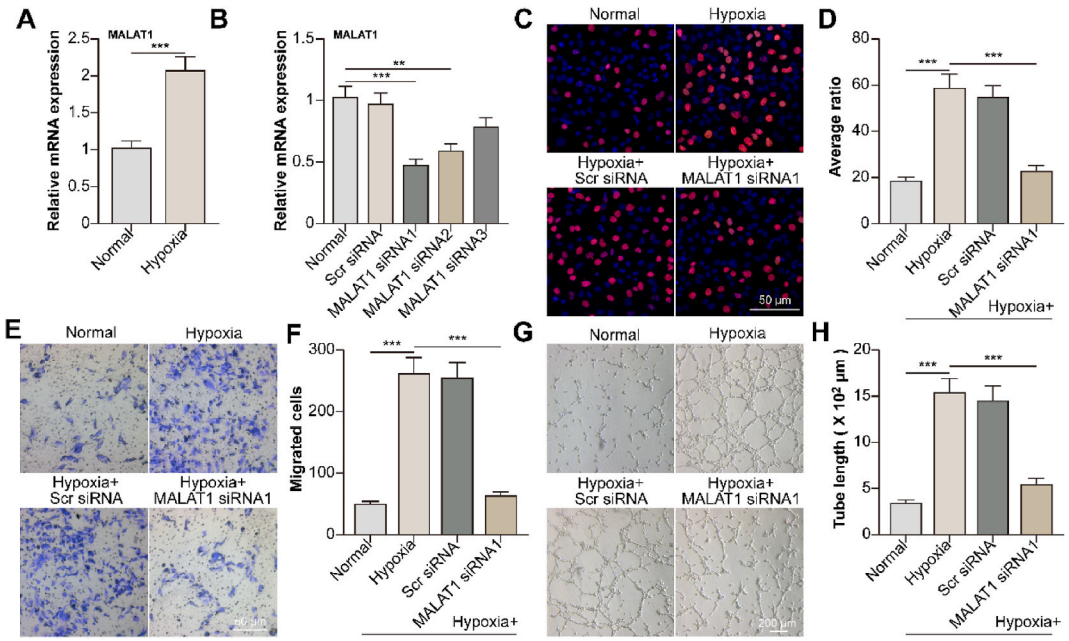

Fig. 2. MALAT1 regulates the function of human choroidal vascular endothelial cells (HCVECs) in vitro. (A). Quantitative real-time polymerase chain reaction (qRT-PCR) was used to determine the mRNA level of MALAT1 in the HCVECs after 24 h of culture in either normoxic or hypoxic conditions. (B). After transfection with MALAT1 small interfering (siRNA) or the negative control, the mRNA level of MALAT1 in HCVECs was identified by qRT-PCR. (C and D). The proliferation of HCVECs was quantified using a 5-ethynyl-20-deoxyuridine assay. Scale bar: 50 μm. (E and F). HCVECs migration was detected using Transwell assay. Scale bar: 50 μm. (G and H). The ability of HCVECs to form tubes was assessed using a tube formation assay.

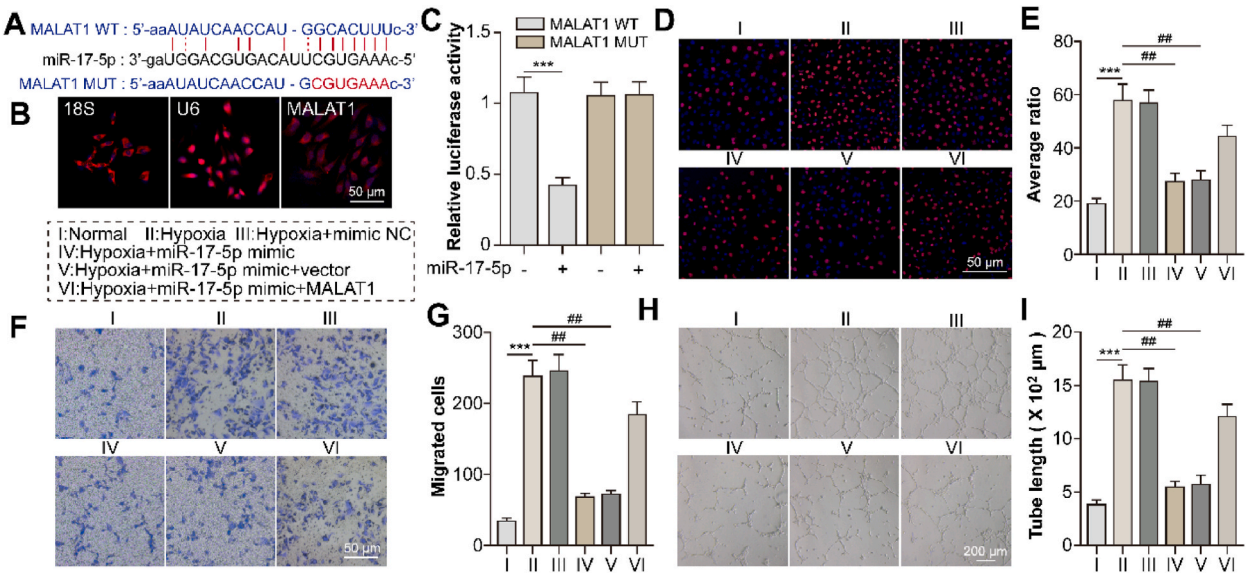

Fig. 3. MALAT1 regulates human choroidal vascular endothelial cells (HCVECs) function by acting as a miR-17-5p sponge.
(A). The MALAT1 and the miR-17-5p binding site were predicted by Starbase. (B). The MALAT1 localization in HCVECs was detected using the fluorescent in situ hybridization assay. The cytoplasmic and nuclear references used were 18S and U6, respectively. Scale bar: 50 μm. (C). The luciferase activity of MALAT1-WT/Mut and miR-17-5p mimic cotransfect in HEK-293T cells. (D and E). The 5-ethynyl-20-deoxyuridine assay was used to evaluate the proliferation of HCVECs. Scale bar: 50 μm. (F and G). A Transwell assay was used to detect HCVECs migration. Scale bar: 50 μm. (H and I). A tube formation assay was used to assess the capacity of HCVECs. Scale bar: 200 μm.

miR-17-5p in HCVECs was then investigated. Under hypoxic conditions, miR-17-5p mimic transfection decreased the proliferation (Fig. 3D–E), migration (Fig. 3F–G), and tube formation (Fig. 3H–I) of HCVECs. HCVECs in the miR-17-5p mimic transfection group proliferation more, migration further, and forming tubes; however, MALAT1 overexpression reversed the miR-17-5p mimic-mediated effects on HCVECs (Fig. 3D–I).

3.4. The MALAT1/miR-17-5p/VEGFA or ETS1 axis is crucial for regulating HCVECs functions

The target gene of miR-17-5p was predicted using Starbase 3.0. Due to their functions in angiogenesis, the candidate genes VEGFA and ETS1 caught our attention (Fig. 4K). VEGFA and ETS1 expression were increased in response to hypoxia, whereas miR-17-5p mimic transfection decreased the mRNA and protein expression of the genes (Fig. 4A–E). MALAT1 knockdown also had a similar effect (Fig. 4F–J).

The downstream of the luciferase gene was used to clone the 3′-UTR of VEGFA and ETS1. The miR-17-5p mimics and luciferase

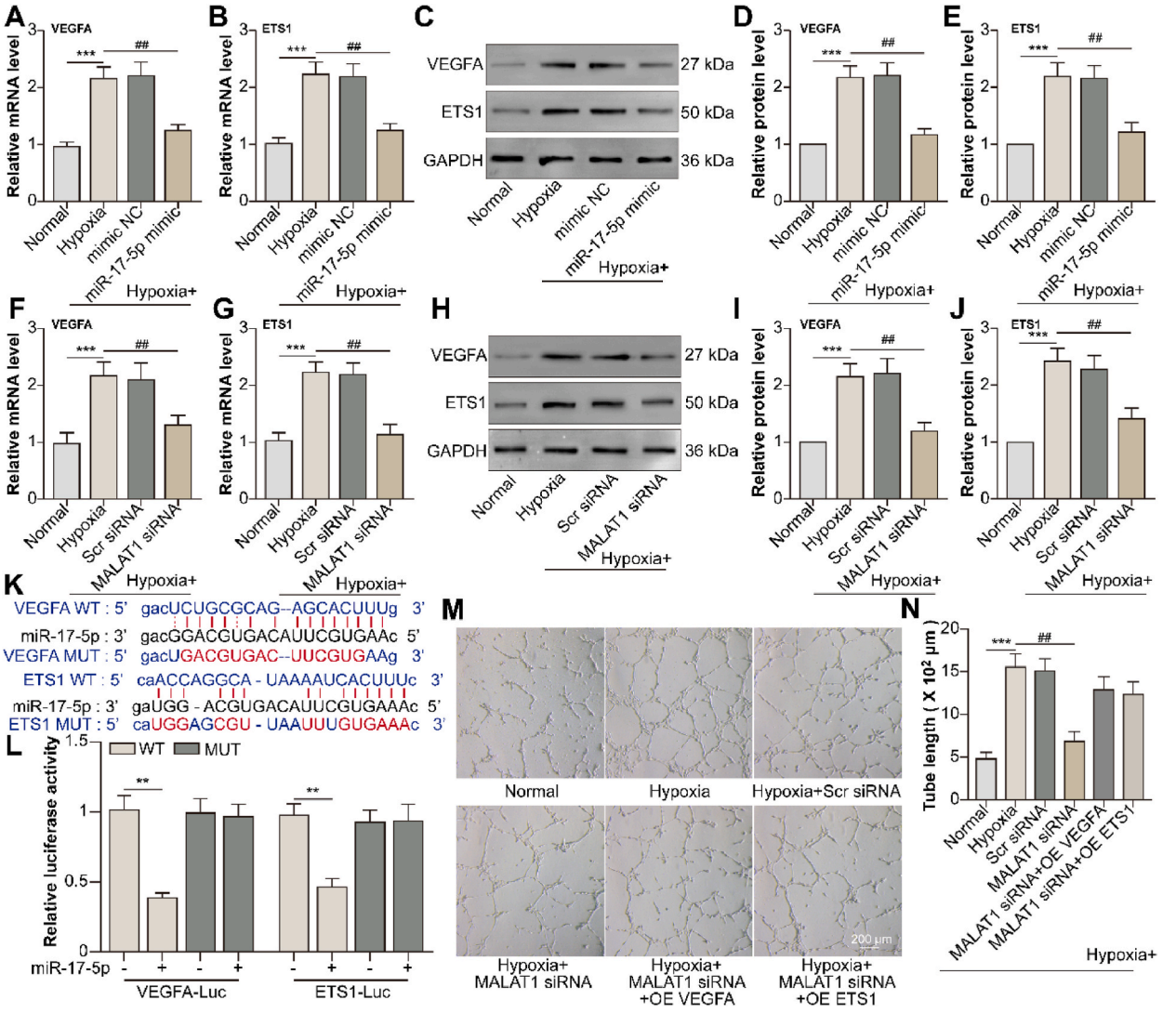

Fig. 4. The MALAT1/miR-17-5p/VEGFA or ETS1 axis is crucial for regulating HCVECs functions. (A). Quantitative real-time polymerase chain reaction (qRT-PCR) was used to determine the mRNA level of VEGFA in HCVECs following transfection with the miR-17-5p mimic. (B). qRT-PCR was used to determine the mRNA level of ETS1 in HCVECs following transfection with miR-17-5p mimic. (C–E). After miR-17-5p mimic transfection, the protein level of VEGFA and ETS1 was detected by Western blot. (F). Following the transfection of MALAT1 small interfering (siRNA), qRT-PCR was used to determine the mRNA level of VEGFA in HCVECs. (G). Following the transfection of MALAT1 siRNA, qRT-PCR was used to determine the mRNA level of ETS1 in HCVECs. (H–J). After MALAT1 siRNA transfection, the protein levels of VEGFA and ETS1 were detected by Western blot. (K). The miR-17-5p binding site for VEGFA or EST1. (L). The co-transfection of VEGFA-WT/Mut or ETS1-WT/Mut with miR-17-5p mimic in HEK-293T cells results in luciferase activity. (M – N). The ability of HCVECs to form tubes was assessed using a tube formation assay. Scale bar: 200 μm.

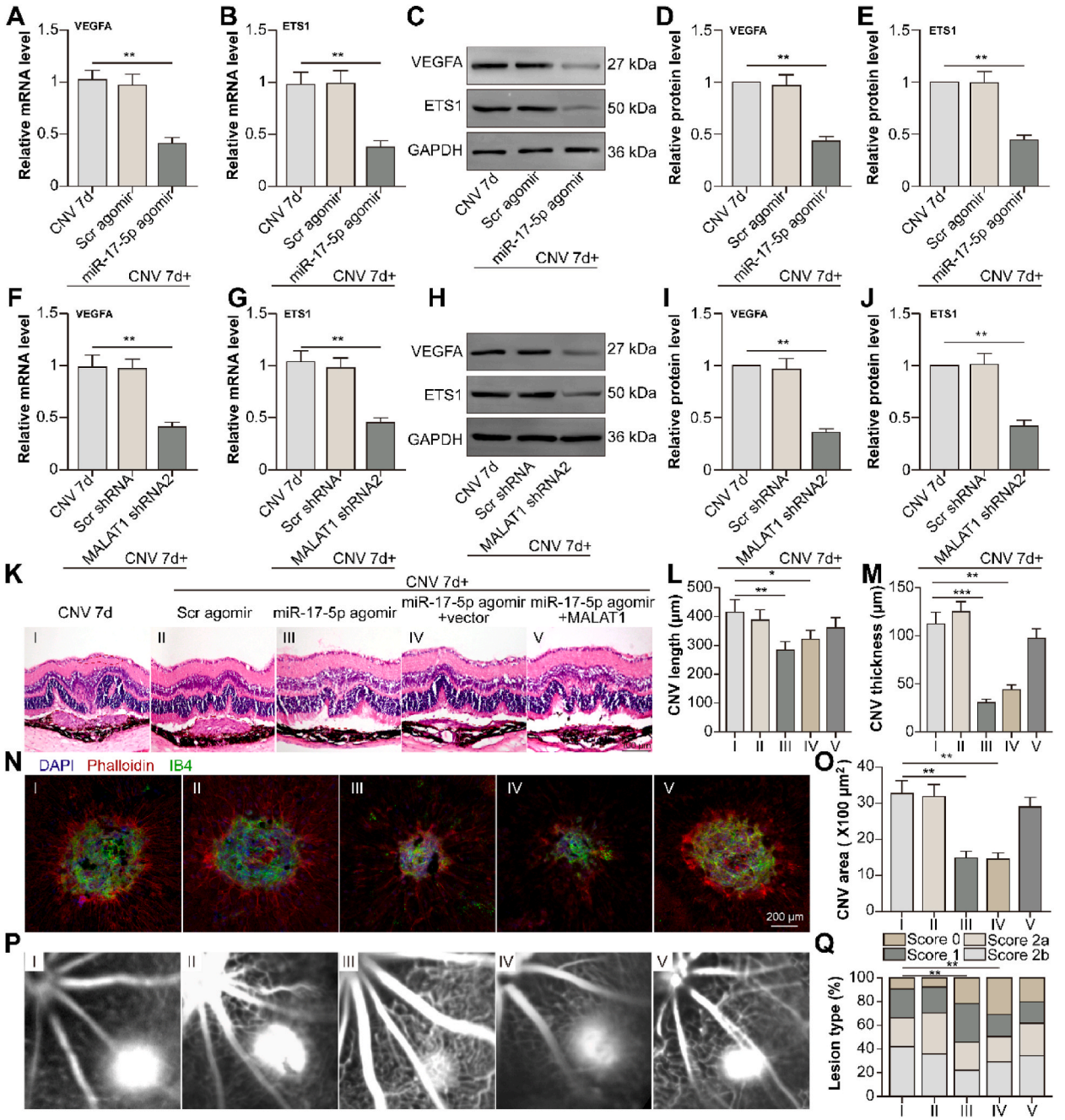

Fig. 5. The MALAT1/miR-17-5p/VEGFA or ETS1 axis is crucial for alleviating mouse laser-induced choroidal neovascularization (CNV) formation. (A). After miR-17-5p agomir transfection, the mRNA level of VEGFA in the retinal pigment epithelial (RPE)-choroidal complexes was detected by quantitative real-time polymerase chain reaction (qRT-PCR). (B). After miR-17-5p agomir transfection, the mRNA level of ETS1 in the RPE-choroidal complexes was detected by qRT-PCR. (C–E). After miR-17-5p agomir transfection, the protein levels of VEGFA and ETS1 were detected by Western blot. (F). After MALAT1 short hairpin RNA (shRNA) transfection, the mRNA level of VEGFA in the RPE-choroidal complexes was detected by qRT-PCR. (G). After MALAT1 shRNA transfection, the mRNA level of ETS1 in the RPE-choroidal complexes was detected by qRT-PCR. (H–J). After MALAT1 shRNA transfection, the protein levels of VEGFA and ETS1 were detected by Western blot. (K). The images of the CNV lesion after hematoxylin and eosin. Scale bar: 100 μm. (L). Measurement of CNV length. (M). Measurement of CNV thickness. (N). Phalloidin and isolectin B4 were used to stain the choroidal flat mounts of CNV mice, and images of the CNV area were obtained using a confocal laser microscope. Scale bar: 200 μm. (O). Measurement of CNV area. (P). After intraperitoneal fluorescein injection, the fundus fluorescein angiography (FFA) images were obtained from the CNV mice. (Q). Graded and quantified angiogenic vessel leakage.

vectors were then co-transfected into HEK-293T cells. Results showed that miR-17-5p mimic transfection significantly decreased luciferase activity, while modification of miR-17-5p binding sites eliminated suppression (Fig. 4L). We also investigated the potential roles of VEGFA and ETS1 in MALAT1-mediated angiogenesis. The Tube formation assay revealed that the hypoxia-induced tube formation was attenuated by MALAT1 knockdown, which was partially reversed by VEGFA and ETS1 overexpression (Fig. 4M–N).

3.5. The MALAT1/miR-17-5p/VEGFA or ETS1 axis is crucial for alleviating mouse laser-induced CNV formation

We then investigated the role of the MALAT1/miR-17-5p/VEGFA or ETS1 axis in the formation of laser-induced CNVs. The results demonstrated that miR-17-5p agomir (Fig. 5A–E) or MALAT1 shRNA (Fig. 5F–J) transfection lowered the mRNA and protein levels of VEGF and ETS1. miR-17-5p agomir increased the thickness and length of CNV lesions in comparison to the control group, according to histopathological analysis. Cotransfecting MALAT1 overexpression plasmids confirmed this (Fig. 5K–M). Immunofluorescence of RPE-choroidal complexes stained with phalloidin and IB-4 revealed that miR-17-5p agomir transfection completely inhibited the area of CNV lesion. MALAT1 overexpression reversed the suppression (Fig. 5N–O). miR-17-5p decreased the vascular leakage of CNV compared to the miR-17-5p scr agomir (negative control) group, while MALAT1 abrogated the protection against vascular leakage provided by miR-17-5p agomir (Fig. 5P–Q) (see Fig. 6).

4. Discussion

LncRNAs may play a role in the progression of AMD, according to certain research [3,14,15]. In this study, we discovered that under hypoxic conditions, MALAT1 expression was increased in RPE-choroidal complexes and HCVECs. Through its role as a miR-17-5p sponge, MALAT1 regulates CNV formation, HCVECs function, and the expression of VEGFA and ETS1.

The participation of VEGF, macrophages, and the change of Bruch's membrane play a crucial role in the formation of CNV. However, CNV is a complex disease, and its development is known to be caused by several stimuli [16]. Different lncRNA expression profiles have been described in early patients with AMD and a laser photocoagulation-induced mice CNV model [15,17]. According to Zhang et al., the RPE-choroidal complexes in the CNV model showed altered expression of 128 lncRNAs. According to GO analysis, angiogenesis was the process in which the altered target genes of the selected lncRNA were most enriched [17]. Several in vitro studies examined the functions of lncRNAs in RPE cells, including BANCR, PWRN2, HDAC4-AS1, ZNF503-AS1, and so on [18–21]. Additionally, researchers have looked into how lncRNAs contribute to CNV. According to Yan et al., IPW expression was significantly upregulated in RPE-choroidal complexes of laser-induced mice model and RF/6A cells cultured in hypoxic conditions. In the mouse model, IPW knockdown inhibited the formation of CNV. The cell viability, proliferation, migration, and tube formation of RF/6A cells in vitro may be inhibited or promoted by IPW silencing or overexpression, respectively [6]. Moreover, Mei et al. reported that miR-148a-3p/PTEN axis increased CNV development via lncRNA NEAT1, and NEAT1 knockdown might suppress CNV by reducing M2 macrophage polarization [3]. We discovered in the current work that MALAT1 was upregulated in choroid tissues after laser photocoagulation and in HCVECs treated in a hypoxic condition. Silencing MALAT1 decreased CNV formation in vivo and in vitro, suggesting MALAT1 is a promising therapeutic target for CNV.

MALAT1 is an endothelial cell-enriched lncRNA, which is regulated by physiological stimuli. The results of the current investigation corroborated previous findings that hypoxia significantly upregulated MALAT1 expression 24 h after exposure [7]. Hemangioma endothelial cells, human umbilical vein endothelial cells, mouse brain microvascular endothelial cells, and other endothelial cells are among the many endothelial cells whose function is regulated by MALAT1 [22–24]. Endothelial cell proliferation, migration, and vasoformation are all inhibited by MALAT1 knockdown [8,22,25]. Additionally, ocular neovascularization, such as diabetic retinopathy, is linked to MALAT1 dysregulation. In high glucose-treated endothelial cells, MALAT1 expression is upregulated, and MALAT1 silencing reduces the proliferation, migration, tube formation, and vascular permeability of retinal vascular endothelial cells [11,26]. MALAT1 knockdown improves diabetes-induced microvascular dysfunction, including loss of pericytes, acellular capillary structure, vascular leakage, and retinal neuroinflammation, in the in vivo model of diabetic retinopathy [10]. This study showed that MALAT1 was upregulated in HCVECs grown in hypoxic conditions and laser-induced mouse CNV model. In vivo CNV formation and leakage were prevented by MALAT1 knockdown, while in vitro HCVEC proliferation, migration, and tube formation capacity were reduced. According to mechanistic studies, MALAT1 regulated the expression of VEGFA and ETS1 by functioning as a miR-17-5p sponge. The information suggests that MALAT1 has a therapeutic impact on CNV.

VEGFA and ETS1 were identified as the target genes for miR-17-5p in the present study. Several ocular neovascular diseases, such as CNV, diabetic retinopathy, retinopathy of prematurity, and neovascular glaucoma, have been linked to VEGFA [27–30]. During the development of the vascular system, the transcription factor ETS1 is recognized to play a critical role in the regulation and differentiation of endothelial cells. According to Casie Chetty S. et al., in embryonic zebrafish, ETS1 promotes endothelial cell survival during vasculogenesis and angiogenesis [31]. Fewer angiogenesis-related genes were expressed by endothelial cells, impairing the development of coronary arteries and reducing cardiomyocyte proliferation in the compact zone [32]. Endothelial cells that were stimulated to invade by VEGF were prevented from doing so by antisense oligonucleotides against ETS [33]. In contrast, ETS1 overexpression boosted the ability of endothelial cells across the Matrigel, along with the upregulation of MMP-1, MMP-3, MMP-9, and integrin-3 [34]. These results revealed that ETS1 had pro-angiogenic properties both in vitro and in vivo. The formation of CNV, a common neovascular disease of the eye, has also been linked to ETS1. In the laser-induced mouse CNV model, the level of ETS1 mRNA was elevated [35]. ETS1 siRNA injected intravitreally decreased CNV leakage and area while lowering RPE dysfunction and macrophage/microglia activation [36]. These observations are consistent with our study, suggesting that ETS1 can be a useful target gene for CNV therapy. However, the specific mechanism by which ETS1 is regulated in CNV is still unknown. This study discovered a novel

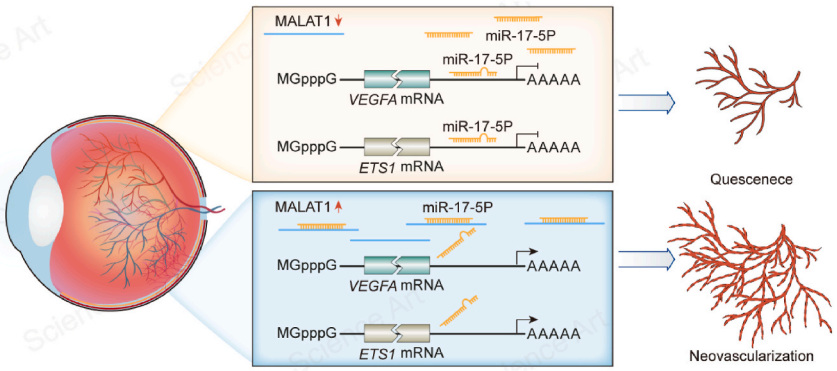

Fig. 6. Schematic overview of the MALAT1 mechanism for aggravating choroidal neovascularization. MALAT1 regulates the expression of VEGFA and ETS1 by acting as a sponge for miR-17-5p.

post-transcriptional mechanism regulating ETS1 by the MALAT1/miR-17-5p axis. MALAT1 regulates the expression of ETS1 by acting as a miR-17-5p sponge.

In conclusion, our findings showed that MALAT1 increased the ability for vasoformation through the miR-17-5p/VEGFA/ETS1 pathway while attenuating CNV formation, suggesting that MALAT1 might be a novel therapeutic target for CNV. However, the expression and function of MALAT1 in this paper have only been validated in mouse models and HCVECs, and there is still a certain distance from clinical application.

Author contribution statement

Xiaoli Zhang, Shu Du, Manhui Zhu: Conceived and designed the experiments; Performed the experiments; Analyzed and interpreted the data; Contributed reagents, materials, analysis tools or data; Wrote the paper.

Defeng Yang: Performed the experiments; Analyzed and interpreted the data.

Xuemei Jin: Performed the experiments; Analyzed and interpreted the data; Contributed reagents, materials, analysis tools or data.

Yuan Zhang: Conceived and designed the experiments; Performed the experiments; Analyzed and interpreted the data; Wrote the paper.

Diya Wang, Huixia Wang: Performed the experiments.

Yan Zhang: Contributed reagents, materials, analysis tools or data.

Funding statement

The study was supported by the project of Jiangsu Provincial Natural Science Foundation {BK20200209}, Gusu Health Talent Program Project in Suzhou {(2022)192} and Suzhou Science and Technology Bureau {SKY20211025, SKJYD2021044}.

Data availability statement

The data used is available in the supplementary material and upon reasonable request.

Declaration of competing interest

The authors declare that they have no conflict of interest.

References

[1] L.F. Hernandez-Zimbron, R. Zamora-Alvarado, L. Ochoa-De la Paz, R. Velez-Montoya, E. Zenteno, R. Gulias-Canizo, H. Quiroz-Mercado, R. Gonzalez-Salinas, Age-related macular degeneration: new paradigms for treatment and management of AMD, Oxid. Med. Cell. Longev. 2018 (2018), 8374647, https://doi.org/10.1155/2018/8374647.

[2] G.J. Jaffe, T.A. Ciulla, A.P. Ciardella, F. Devin, P.U. Dugel, C.M. Eandi, H. Masonson, J. Mones, J.A. Pearlman, M. Quaranta-El Maftouhi, F. Ricci, K. Westby, S. C. Patel, Dual antagonism of pdgf and VEGF in neovascular age-related macular degeneration: a phase IIb, multicenter, randomized controlled trial, Ophthalmology 124 (2017) 224–234, https://doi.org/10.1016/j.ophtha.2016.10.010.

[3] P. Zhang, B. Lu, Q. Zhang, F. Xu, R. Zhang, C. Wang, Y. Liu, C. Wei, L. Mei, LncRNA NEAT1 sponges MiRNA-148a-3p to suppress choroidal neovascularization and M2 macrophage polarization, Mol. Immunol. 127 (2020) 212–222, https://doi.org/10.1016/j.molimm.2020.08.008.

[4] L. Zhang, H. Zeng, J.H. Wang, H. Zhao, B. Zhang, J. Zou, S. Yoshida, Y. Zhou, Altered long non-coding RNAs involved in immunological regulation and associated with choroidal neovascularization in mice, Int. J. Med. Sci. 17 (2020) 292–301, https://doi.org/10.7150/ijms.37804.

[5] Y. Zhang, S. Cai, Y. Jia, C. Qi, J. Sun, H. Zhang, F. Wang, Y. Cao, X. Li, Decoding noncoding RNAs: role of MicroRNAs and long noncoding RNAs in ocular neovascularization, Theranostics 7 (2017) 3155–3167, https://doi.org/10.7150/thno.19646.

[6] T.J. Yang, M.D. Yao, Y.N. Sun, X.M. Li, Q. Jiang, B. Yan, Suppression of choroidal neovascularization by silencing of long non-coding RNA IPW, Aging (Albany NY) 13 (2021) 10584–10602, https://doi.org/10.18632/aging.202822.

[7] K.M. Michalik, X. You, Y. Manavski, A. Doddaballapur, M. Zornig, T. Braun, D. John, Y. Ponomareva, W. Chen, S. Uchida, R.A. Boon, S. Dimmeler, Long noncoding RNA MALAT1 regulates endothelial cell function and vessel growth, Circ. Res. 114 (2014) 1389–1397, https://doi.org/10.1161/CIRCRESAHA.114.303265.

[8] Q. Li, X. Liu, W. Liu, Y. Zhang, M. Wu, Z. Chen, Y. Zhao, L. Zou, MALAT1 sponges miR-26a and miR-26b to regulate endothelial cell angiogenesis via PFKFB3-driven glycolysis in early-onset preeclampsia, Mol. Ther. Nucleic Acids 23 (2021) 897–907, https://doi.org/10.1016/j.omtn.2021.01.005.

[9] Y. Li, Z. Wu, J. Yuan, L. Sun, L. Lin, N. Huang, J. Bin, Y. Liao, W. Liao, Long non-coding RNA MALAT1 promotes gastric cancer tumorigenicity and metastasis by regulating vasculogenic mimicry and angiogenesis, Cancer Lett. 395 (2017) 31–44, https://doi.org/10.1016/j.canlet.2017.02.035.

[10] J.Y. Liu, J. Yao, X.M. Li, Y.C. Song, X.Q. Wang, Y.J. Li, B. Yan, Q. Jiang, Pathogenic role of lncRNA-MALAT1 in endothelial cell dysfunction in diabetes mellitus, Cell Death Dis. 5 (2014) e1506, https://doi.org/10.1038/cddis.2014.466.

[11] A. Tan, T. Li, L. Ruan, J. Yang, Y. Luo, L. Li, X. Wu, Knockdown of Malat1 alleviates high-glucose-induced angiogenesis through regulating miR-205-5p/VEGF-A axis, Exp. Eye Res. 207 (2021), 108585, https://doi.org/10.1016/j.exer.2021.108585.

[12] N. Lara-Castillo, S. Zandi, S. Nakao, Y. Ito, K. Noda, H. She, M. Ahmed, S. Frimmel, Z. Ablonczy, A. Hafezi-Moghadam, Atrial natriuretic peptide reduces vascular leakage and choroidal neovascularization, Am. J. Pathol. 175 (2009) 2343–2350, https://doi.org/10.2353/ajpath.2009.090439.

[13] Y. Tay, J. Rinn, P.P. Pandolfi, The multilayered complexity of ceRNA crosstalk and competition, Nature 505 (2014) 344–352, https://doi.org/10.1038/nature12986.

[14] S. Hagbi-Levi, M. Grunin, T. Jaouni, L. Tiosano, B. Rinsky, S. Elbaz-Hayoun, A. Peled, I. Chowers, Proangiogenic characteristics of activated macrophages from patients with age-related macular degeneration, Neurobiol. Aging 51 (2017) 71–82, https://doi.org/10.1016/j.neurobiolaging.

[15] W. Zhu, Y.F. Meng, Q. Xing, J.J. Tao, J. Lu, Y. Wu, Identification of lncRNAs involved in biological regulation in early age-related macular degeneration, Int. J. Nanomed. 12 (2017) 7589–7602, https://doi.org/10.2147/IJN.S140275.

[16] Y.J. Yu, B. Mo, L. Liu, Y.K. Yue, C.L. Yue, W. Liu, Inhibition of choroidal neovascularization by lentivirus-mediated PEDF gene transfer in rats, Int. J. Ophthalmol. 9 (2016) 1112–1120, https://doi.org/10.18240/ijo.2016.08.05.

[17] P. Zhang, B. Lu, F. Xu, C. Wang, R. Zhang, Y. Liu, C. Wei, L. Mei, Analysis of long noncoding RNAs in choroid neovascularization, Curr. Eye Res. 45 (2020) 1403–1414, https://doi.org/10.1080/02713683.2020.1748659.

[18] R.K. Kutty, W. Samuel, T. Duncan, O. Postnikova, C. Jaworski, C.N. Nagineni, T.M. Redmond, Proinflammatory cytokine interferon-gamma increases the expression of BANCR, a long non-coding RNA, in retinal pigment epithelial cells, Cytokine 104 (2018) 147–150, https://doi.org/10.1016/j.cyto.2017.10.009.

[19] X. Yu, Y. Luo, G. Chen, H. Liu, N. Tian, X. Zen, Y. Huang, Long non-coding RNA PWRN2 regulates cytotoxicity in an in vitro model of age-related macular degeneration, Biochem. Biophys. Res. Commun. 535 (2021) 39–46, https://doi.org/10.1016/j.bbrc.2020.10.104.

[20] J. Pan, L. Zhao, Long non-coding RNA histone deacetylase 4 antisense RNA 1 (HDAC4-AS1) inhibits HDAC4 expression in human ARPE-19 cells with hypoxic stress, Bioengineered 12 (2021) 2228–2237, https://doi.org/10.1080/21655979.2021.1933821.

[21] X. Chen, C. Jiang, B. Qin, G. Liu, J. Ji, X. Sun, M. Xu, S. Ding, M. Zhu, G. Huang, B. Yan, C. Zhao, LncRNA ZNF503-AS1 promotes RPE differentiation by downregulating ZNF503 expression, Cell Death Dis. 8 (2017), e3046, https://doi.org/10.1038/cddis.2017.382.

[22] S. Wang, L. Ren, G. Shen, M. Liu, J. Luo, The knockdown of MALAT1 inhibits the proliferation, invasion and migration of hemangioma endothelial cells by regulating MiR-206/VEGFA axis, Mol. Cell. Probes 51 (2020), 101540, https://doi.org/10.1016/j.mcp.2020.101540.

[23] Y.-W.Z. Yu-Ping Gong, Xiao-Qing Su1, Hai-Bo Gao, Inhibition of long noncoding RNA MALAT1 suppresses high glucose-induced apoptosis and inflammation in human umbilical vein endothelial cells by suppressing the NF-κB signaling pathway, Biochem. Cell. Biol. 98 (2020) 669–675, https://doi.org/10.1139/bcb-2019-0403.

[24] S. Wang, X. Han, Z. Mao, Y. Xin, S. Maharjan, B. Zhang, MALAT1 lncRNA induces autophagy and protects brain microvascular endothelial cells against oxygen-glucose deprivation by binding to miR-200c-3p and upregulating SIRT1 expression, Neuroscience 397 (2019) 116–126, https://doi.org/10.1016/j.neuroscience.2018.11.024.

[25] C. Wang, Y. Qu, R. Suo, Y. Zhu, Long non-coding RNA MALAT1 regulates angiogenesis following oxygen-glucose deprivation/reoxygenation, J. Cell Mol. Med. 23 (2019) 2970–2983, https://doi.org/10.1111/jcmm.14204.

[26] Y. Wang, L. Wang, H. Guo, Y. Peng, D. Nie, J. Mo, L. Ye, Knockdown of MALAT1 attenuates high-glucose-induced angiogenesis and inflammation via endoplasmic reticulum stress in human retinal vascular endothelial cells, Biomed. Pharmacother. 124 (2020), 109699, https://doi.org/10.1016/j.biopha.2019.109699.

[27] M. Lu, A.P. Adamis, Molecular biology of choroidal neovascularization, Ophthalmol Clin North Am 19 (2006) 323–334, https://doi.org/10.1016/j.ohc.2006.05.001.

[28] N. Cheung, I.Y. Wong, T.Y. Wong, Ocular anti-VEGF therapy for diabetic retinopathy: overview of clinical efficacy and evolving applications, Diabetes Care 37 (2014) 900–905, https://doi.org/10.2337/dc13-1990.

[29] L.J. Tripathi Rc, B.J. Tripathi, K.V. Chalam, A.P. Adamis, Increased level of vascular endothelial growth factor in aqueous humor of patients with neovascular glaucoma, Ophthalmology 105 (1998) 232–237, https://doi.org/10.1016/s0161-6420(98)92782-8.

[30] Y. Guo, F. Du, Y.L. Tan, J. Luo, D. Xiong, W.T. Song, VEGF-mediated angiogenesis in retinopathy of prematurity is co-regulated by miR-17-5p and miR-20a-5p, Biochem. Cell. Biol. 99 (2021) 414–423, https://doi.org/10.1139/bcb-2020-0357.

[31] S. Casie Chetty, S. Sumanas, Ets1 functions partially redundantly with Etv2 to promote embryonic vasculogenesis and angiogenesis in zebrafish, Dev. Biol. 465 (2020) 11–22, https://doi.org/10.1016/j.ydbio.2020.06.007.

[32] L. Wang, L. Lin, H. Qi, J. Chen, P. Grossfeld, Endothelial loss of ETS1 impairs coronary vascular development and leads to ventricular non-compaction, Circ. Res. 131 (2022) 371–387, https://doi.org/10.1161/CIRCRESAHA.121.319955.

[33] Z.F.R. Chen, C.W. Riggs, J.S. Rhim, J.A. Lautenberger, Inhibition of vascular endothelial growth factor-induced endothelial cell migration by ETS1 antisense oligonucleotides, Cancer Res. 57 (1997) 2013. –2019.

[34] M.A. N Oda, Y. Sato, ETS-1 converts endothelial cells to the angiogenic phenotype by inducing the expression of matrix metalloproteinases and integrin beta3, J. Cell. Physiol. 178 (1999) 121–132, 10.1002/(SICI)1097-4652(199902)178:2<121::AID-JCP1>3.0.CO;2-F.

[35] S. Kinoshita, K. Noda, Y. Tagawa, S. Inafuku, Y. Dong, J. Fukuhara, Z. Dong, R. Ando, A. Kanda, S. Ishida, Genistein attenuates choroidal neovascularization, J. Nutr. Biochem. 25 (2014) 1177–1182, https://doi.org/10.1016/j.jnutbio.2014.06.004.

[36] M. Zhu, L. Jiang, Y. Yuan, L. Chen, X. Liu, J. Liang, Q. Zhu, D. Ding, E. Song, Intravitreal Ets1 siRNA alleviates choroidal neovascularization in a mouse model of age-related macular degeneration, Cell Tissue Res. 376 (2019) 341–351, https://doi.org/10.1007/s00441-019-03001-1.